Closed-Loop Control Design for a Three-Level Three-Phase Neutral-Point-Clamped Inverter Using the Optimized Nearest-Three Virtual-Space-Vector Modulation

S. Busquets-Monge[1], J. D. Ortega[1], J. Bordonau[1], J. A. Beristáin[2], and J. Rocabert[1]

[1] Dept. of Electronic Engineering
Technical University of Catalonia
Av. Diagonal 647
08028 Barcelona, Spain
Email: sergio.busquets@upc.edu

[2] Dept. of Electrical and Electronic Engineering
Instituto Tecnológico de Sonora
5 de febrero 818, 85000
Ciudad Obregón, Sonora, Mexico
Email: bantonio@itson.mx

***Abstract*— This paper presents a closed-loop control scheme for the three-level three-phase neutral-point-clamped dc-ac converter using the optimized nearest-three virtual-space-vector pulsewidth modulation, a modulation that produces a low output voltage distortion with a significant reduction of the dc-link capacitance. A specific loop modifying the modulating waveforms is introduced to rapidly control possible perturbations in the neutral-point voltage balance. The remaining part of the control is analogous to the control for a two-level converter with an appropriate interfacing to the selected modulation, including an online estimation of the load displacement angle at no extra cost. The closed-loop control is designed for the case of a renewable energy source connected to the ac mains and its performance is analyzed through simulation and experiments.**

I. INTRODUCTION

Multilevel converter topologies [1]-[2] have received special attention during the last two decades due to their significant advantages in high-power medium-and-high-voltage applications. In these topologies, and compared to a two-level converter, the voltage across each semiconductor is reduced, avoiding the problems of the series interconnection of devices, reducing the harmonic distortion of the output voltage, and improving the efficiency. But a larger number of semiconductors are needed and the modulation strategy to control them becomes more complex.

Among these topologies, the three-level three-phase neutral-point-clamped (NPC) dc-ac converter [3], in Fig. 1(a), is probably the most popular. The application of conventional modulation techniques to this converter causes a low frequency (around three times the fundamental frequency of the output voltage, f_o) oscillation of the neutral-point voltage. This, in turn, increases the voltage stress on the devices and generates low order harmonics in the output voltage.

There have been many efforts to analyze this problem and define a modulation strategy to solve it [4]-[14], therefore eliminating the need to significantly increase the dc-side capacitance to minimize the voltage oscillation. Among them, the nearest-three virtual-space-vector (NTV^2) pulsewidth modulation (PWM) [13], allows controlling the neutral-point voltage over the full range of converter output voltage and for any load. The optimized nearest-three virtual-space-vector (ONTV^2) PWM [14] also allows comprehensively controlling the neutral-point voltage but with a lower output voltage harmonic distortion in the case of linear-and-balanced ac loads.

The design of a closed-loop control scheme interfacing the ONTV^2 PWM and correcting possible dc-link capacitor voltage balance perturbations is not straightforward. This paper presents a proposal for such control, focusing on a particular application, and the performance of the proposed control scheme is verified through simulation and experiments.

II. OPTIMIZED NEAREST-THREE VIRTUAL-SPACE-VECTOR PWM

Let us designate d_{ap}, d_{bp}, d_{cp}, d_{an}, d_{bn}, d_{cn} the six independent converter phase duty-ratios, where d_{xy} refers to the duty ratio of the phase x connection to the dc-link point y. Equation (1) reproduces from [14] the six expressions that define the ONTV^2 PWM in terms of these six independent converter phase duty-ratios in *d-q-0* coordinates (d_{pd}, d_{pq}, d_{p0}, d_{nd}, d_{nq}, d_{n0}).

$$
\begin{aligned}
&d_{pd} = \tan(\varphi)\cdot d_{pq} + m/\sqrt{2}\\
&d_{nd} = d_{pd} - \sqrt{2}\cdot m\\
&d_{nq} = d_{pq}\\
&\begin{cases}
\theta \le 2\pi/3: \;\; d_{p0} = \sqrt{2}\cdot\left(-d_{pd}\cdot\cos(\theta+2\pi/3) + d_{pq}\cdot\sin(\theta+2\pi/3)\right)\\
2\pi/3 < \;\theta \le 4\pi/3: \;\; d_{p0} = \sqrt{2}\cdot\left(-d_{pd}\cdot\cos(\theta) + d_{pq}\cdot\sin(\theta)\right)\\
\theta > 4\pi/3: \;\; d_{p0} = \sqrt{2}\cdot\left(-d_{pd}\cdot\cos(\theta-2\pi/3) + d_{pq}\cdot\sin(\theta-2\pi/3)\right)
\end{cases}\\
&\begin{cases}
\theta \le \pi/3,\ \theta > 5\pi/3: \;\; d_{n0} = \sqrt{2}\cdot\left(-d_{nd}\cdot\cos(\theta) + d_{nq}\cdot\sin(\theta)\right)\\
\pi/3 < \theta \le \pi: \;\; d_{n0} = \sqrt{2}\cdot\left(-d_{nd}\cdot\cos(\theta-2\pi/3) + d_{nq}\cdot\sin(\theta-2\pi/3)\right)\\
\pi < \theta \le 5\pi/3: \;\; d_{n0} = \sqrt{2}\cdot\left(-d_{nd}\cdot\cos(\theta+2\pi/3) + d_{nq}\cdot\sin(\theta+2\pi/3)\right)
\end{cases}\\
&d_{pq} = -K\cdot\sin(3\theta)
\end{aligned}
\qquad (1)
$$

where m ($\in$ [0, 1]) and θ are the length and angle (with reference to axis α, aligned with vector $\mathbf{V}_{L1}$ corresponding to switching state *pnn* [13]) of the reference vector, $\mathbf{V}_{ref}$, a rotating vector in the converter space vector plane that represents the desired fundamental converter output three-phase voltage. The expressions in (1) assume that axis *d* of the *d-q-0* transformation of the phase duty-ratios is aligned with $\mathbf{V}_{ref}$. Variable φ is the ac load/source displacement angle and the optimum value of parameter K is a function of m and φ. In [14], expressions are provided to compute the value of K as a function of m and φ. Alternatively, a look-up table as a function of m and $\tan(\varphi)$ can be generated to select the appropriate value of K on-line.

Given the values of m, θ, and $\tan(\varphi)$, the duty ratios in *d-q-0* coordinates can be obtained from (1) and the look-up table or expressions to compute K. Applying the inverse

d-q-0 transformation, we then obtain the independent phase duty-ratios d_{ap}, d_{bp}, d_{cp}, d_{an}, d_{bn}, d_{cn}. From these duty ratios and assuming that the sequence within a switching cycle of connection of each phase to each of the dc-link points is the symmetrical *p-o-n-o-p*, it is fairly straightforward to generate the twelve switch control signals.

III. Closed-Loop Control Design

The proposed modulator and controller have been designed and implemented for the particular system in Fig. 1(a). The purpose of the system is to send the energy from a renewable energy source to the mains with unity power factor while also regulating voltage v_{pn}. The closed-loop control designed is applicable to any system where the power source can be basically modeled as a current source and the energy is sent to the mains, such as, for example, a wind energy conversion system where the ac generator is connected to a non-controlled boost rectifier. The diagrams of Fig. 1(b) and Fig. 1(c) summarize the proposed controller and modulator structure, discussed in detail next.

A. Neutral-Point Voltage Control

The ONTV^2 PWM guarantees no low-frequency oscillations of v_{unb} due to the loading conditions of the converter provided that the addition of line currents equals zero. Even if the load presents a severe non-linearity, this will not affect the dc-link voltage balance if we set $K = 0$. The occurrence of neutral-point voltage perturbations should however be considered. Perturbations can occur if, for example, there is a leakage current flowing from the load neutral to ground, causing that the addition of the three-phase currents be different from zero. The non-idealities, and specially the differences, in the switching behavior of the converter devices are another possible source of disturbances.

As discussed in [15], certain modulations have the property of naturally recovering the dc-link voltage balance after a perturbation. The ONTV^2 PWM with $K = 0$ does not belong to this family of modulations. It does not affect the balance of the dc-link capacitors. If an unbalance exists at a given point in time, the ONTV^2 PWM with $K = 0$ will preserve this unbalance (see Fig. 2(a)). However, the ONTV^2 with $K > 0$ does belong to the set of modulations that naturally recover the balance (see Fig. 2(b)). The higher the value of K, the faster the system recovers the balance. Still, this natural recovery process is usually slow.

The addition of discharging resistors to the dc-link capacitors also helps recovering the balance after a perturbation. Their resistance value is usually high, though, and the recovery process thanks to these resistors is also slow.

Since all preexisting possible balance recovery processes do not seem to be effective/fast enough, an appropriate perturbation of the modulating waveforms that allowed speeding-up this process would be helpful. Reference [7] shows that introducing a common-mode voltage into all three line-to-neutral output-voltage waveforms causes an unbalance in the discharging of the dc-link capacitors. This property can be used to speed-up the recovery process whenever a dc-link voltage unbalance occurs. Here, this control mechanism is adapted to the ONTV^2 PWM, leading to an alternative scheme to guarantee the dc-link capacitor voltage balance in the three-level three-phase NPC dc-ac converter different from other solutions presented [16].

The introduction of a common mode voltage can be done by adding an offset (d_{offset}) to all three d_{ap}–d_{an}, d_{bp}–d_{bn}, d_{cp}–d_{cn} modulating waveforms. If we want to add an offset to the d_{ap}–d_{an} waveform, we have three options:

1) We add the offset to d_{ap}.
2) We subtract the offset from d_{an}.
3) We add part of the offset to d_{ap} and we subtract the remaining part from d_{an}.

A simple and interesting strategy is to apply all the offset to the duty ratio to be reduced. Since duty ratios must be greater than zero, in case we reach the value of zero, the other duty ratio will be increased an amount corresponding to the part of the offset still not applied. This strategy allows minimizing the number of commutations, since it will maximize the occasions where a non-zero duty-ratio becomes zero. With reference to Fig. 1(c), this strategy can be formulated for phase x as

$$d'_{ap} = f_{61}(d_{ap}, d_{an}, d_{\text{offset}});\ d'_{an} = f_{62}(d_{ap}, d_{an}, d_{\text{offset}});$$
$$d'_{bp} = f_{63}(d_{bp}, d_{bn}, d_{\text{offset}});\ d'_{bn} = f_{64}(d_{bp}, d_{bn}, d_{\text{offset}});$$
$$d'_{cp} = f_{65}(d_{cp}, d_{cn}, d_{\text{offset}});\ d'_{cn} = f_{66}(d_{cp}, d_{cn}, d_{\text{offset}});$$

```
if (d_offset ≥ 0) {
   if (d_xn > d_offset) {
      d'_xn = d_xn − d_offset
      d'_xp = d_xp
   }else {
      d'_xn = 0
      d'_xp = d_xp + (d_offset − d_xn)
   }
}else {
   if (d_xp > | d_offset |) {
      d'_xp = d_xp − | d_offset |
      d'_xn = d_xn
   }else {
      d'_xp = 0
      d'_xn = d_xn + (|d_offset | − d_xp)
   }
}
```

(2)

The value of d_{offset} to be applied is determined from the dc-link capacitor voltage unbalance $v_{\text{unb}} = f_{11}(v_{C1}, v_{C2}) = = (v_{C2} - v_{C1}) / 2$ by a compensator. This compensator must have a low-pass characteristic, in order to only react to perturbations in the dc-link voltage balance with frequencies lower than the switching frequency.

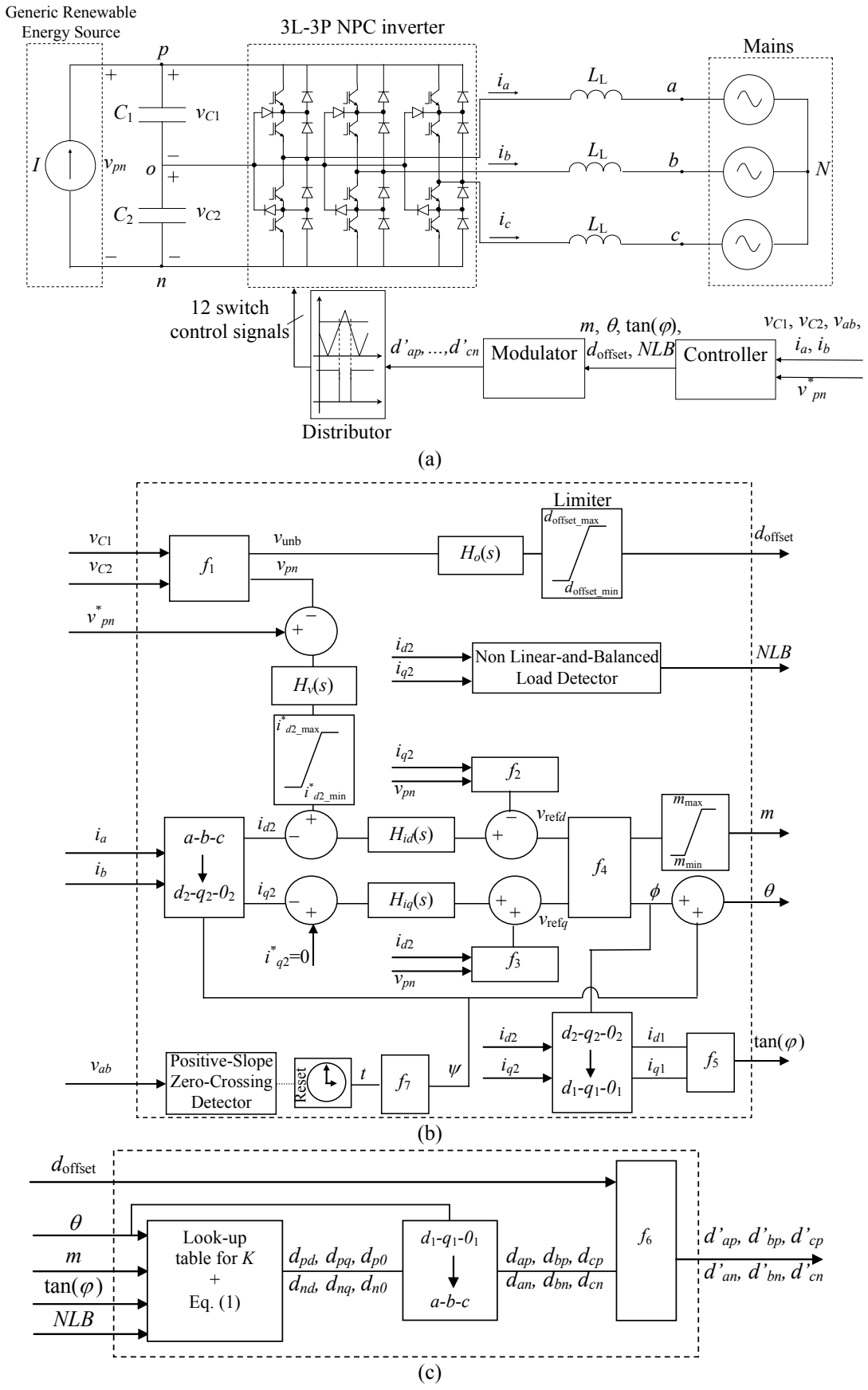

Fig. 1. System block diagram. (a) Power stage plus control. (b) Controller structure. (c) Modulator structure.

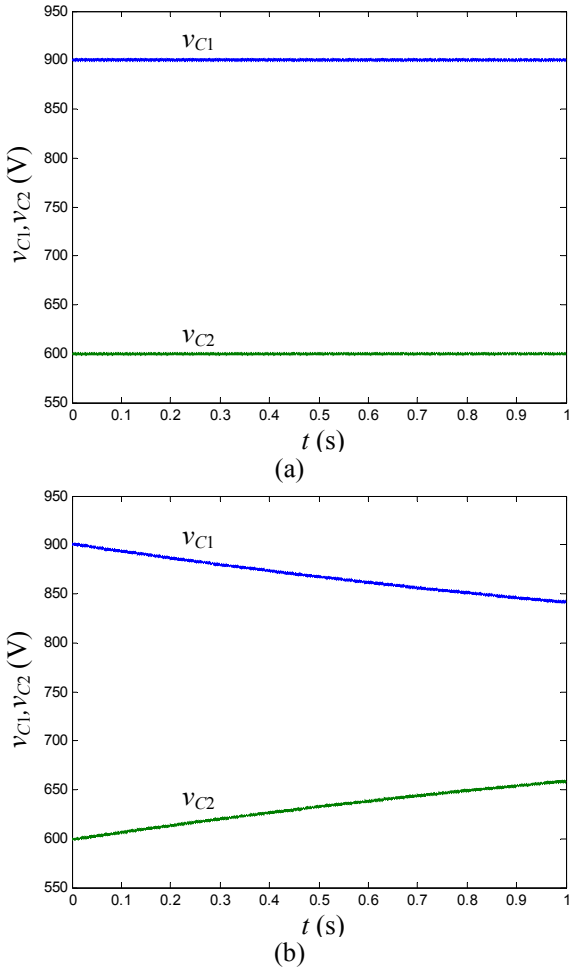

Fig. 2. Natural dc-link capacitor voltage balance recovery transient in the following conditions: V_{pn} = 1500 V, m = 0.75, f_o = 50 Hz, switching frequency f_s = 5 kHz, $C_1 = C_2$ = 1 mF, and a wye connected three-phase R-L load (R_L = 10 Ω, L_L = 10 mH). (a) ONTV^2 PWM, K = 0. (b) ONTV^2 PWM, K = 0.09.

B. Non Linear-and-Balanced Load Detector

Whenever the load is not linear and balanced, we must set $K = 0$ in order to maintain the neutral-point voltage control. This situation can be detected by monitoring the maximum length of the line-current vector oscillation in d-q coordinates, and if it goes beyond a given maximum, activating and latching a non linear-and-balanced load flag (*NLB*) in order to force $K = 0$ in the modulator.

C. Reference Vector Computation

From a closed-loop control point of view, the key difference between a two-level and a three-level dc-ac converter is that the latter introduces the dynamics of the neutral-point voltage. We can assume that the neutral-point voltage is always balanced thanks to the chosen modulation and the dedicated control presented above. Then, the average model of the three-level converter becomes equivalent to the model of a two-level converter. Hence, conventional control schemes and design procedures for the two-level converter can be directly applied to the three-level converter to obtain, from the sensed variables, the reference vector length m and angle θ required by the modulator.

For the particular application considered here, the selected control scheme is shown in Fig. 1(b). First, the dc-link voltage $v_{pn} = f_{12}(v_{C1}, v_{C2}) = v_{C1} + v_{C2}$ is compared to the desired command. The error is then processed by a compensator to produce the i_d command. Line currents i_a and i_b are sensed and d-q transformed. We do not need to sense i_c since we know $i_c = -i_a - i_b$. The transformation is performed to axes d_2-q_2-0_2, where axis d_2 is in phase with the vector of line-to-neutral mains voltages ($\mathbf{V}_{L\text{-}N}$). This vector has an angle ψ with reference to axis α (Fig. 3):

$$\psi = f_7(t) = \omega_o \cdot t - 2\pi/3 = 2\pi \cdot f_o - 2\pi/3. \tag{3}$$

The d_2 and q_2 components of the current are compared to their corresponding command. The i_{q2} command is zero to achieve a unity displacement factor for the power transferred to the mains. Both d and q channel errors are processed by their specific compensators. Finally, both channels are decoupled through f_2 and f_3:

$$\begin{aligned} f_2(i_{q2}, v_{pn}) &= \left(\sqrt{2} \cdot i_{q2} \cdot \omega_o \cdot L_L\right) / v_{pn} \\ f_3(i_{d2}, v_{pn}) &= \left(\sqrt{2} \cdot i_{d2} \cdot \omega_o \cdot L_L\right) / v_{pn}. \end{aligned} \tag{4}$$

The outcome of both channels is the d_2 and q_2 components of $\mathbf{V}_{ref}$. Through f_4 we obtain the $\mathbf{V}_{ref}$ length m (modulation index) and angle ϕ (with reference to axis d_2):

$$\begin{aligned} m &= f_{41}(v_{refd}, v_{refq}) = \sqrt{v_{refd}^2 + v_{refq}^2} \\ \phi &= f_{42}(v_{refd}, v_{refq}) = \tan^{-1}(v_{refq} / v_{refd}). \end{aligned} \tag{5}$$

Angle θ can then be obtained by simply adding ψ and ϕ (Fig. 3). This is the angle that will be used to perform the transformation of the duty ratios from d_1-q_1-0_1 to a-b-c coordinates within the modulator.

D. Online Estimation of tan(φ)

To implement the ONTV^2 PWM we need an estimate of tan(φ). Angle φ corresponds to the angle between the vector of fundamental line currents and $\mathbf{V}_{ref}$. Hence, the value of tan(φ) can be computed online by simply sensing the line currents, applying the d_1-q_1 transformation, and using (6) (in the case of non linear-and-balanced loads, the dc values of the d_1 and q_1 components can be used). Since, in general, the controller already requires sensing the line currents, the implementation of the ONTV^2 PWM does not require additional sensors.

$$\tan(\varphi) = f_5(i_{d1}, i_{q1}) = -i_{q1} / i_{d1}. \tag{6}$$

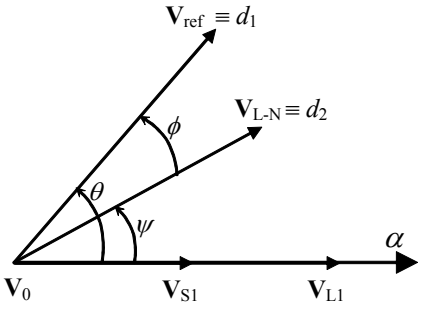

Fig. 3. Location of vectors $\mathbf{V}_{ref}$ and $\mathbf{V}_{L\text{-}N}$ with reference to axis α.

IV. SIMULATION AND EXPERIMENTAL RESULTS

Simulations have been carried out in Simulink with closed-loop switching and average models of the system. For the experimental validation, the controller and modulator blocks have been implemented using a PowerPC (dSPACE 1103) and the distributor block using a FPGA (Altera EPF10K70).

Fig. 4(a) demonstrates the advantage of introducing the neutral-point voltage control. The simulation has been performed in the same conditions as in Fig. 2(a). Fig 4(b) shows the perturbed duty-ratio pattern during the transient. Fig. 5 depicts the good performance achieved with this control in the experiments. In Fig. 5(a), the control effort is negligible: $d_{\text{offset}} \cong -0.001$. In Fig. 5(b), $d_{\text{offset}} \cong -0.01$.

The complete control has been tested through simulation in the conditions of Fig. 6. These results have been obtained with the complete closed-loop switching model for a step in voltage command v^*_{pn} from 800 V to 750 V. We can observe that there is no unbalance of the dc-link capacitor voltages before, during, and after the step transient, as expected (Fig. 6(a)). Since the ONTV^2 PWM already guarantees this balancing, the effort of the dedicated control is minimal ($-0.001 < d_{\text{offset}} < 0.001$). In Fig. 6(b) we can observe that the power conversion is achieved with unity displacement factor, as intended.

Fig. 7 shows the experimental results obtained with an emulator of a wind energy conversion system connected to the ac mains (Fig. 1(a)). The voltage of a wind mill generator is connected to the inverter dc-link through a set of three line inductances (L_S) and a three-phase diode rectifier. A constant torque of 10 Nm is applied to the generator shaft to emulate the wind torque. A step in v^*_{pn} from 340 V to 300 V is forced, producing a variation of the rotor speed from 1577 rpm to 1396 rpm. The controller employed is defined in (7).

The results show an overall good performance of the complete control, which guarantees the dc-link capacitor voltage balance and unity displacement factor during the entire transient.

$$
\begin{aligned}
H_o(s) &= -2 \cdot \frac{(s + 2\pi \cdot 0.01)}{s \cdot (s + 2\pi \cdot 25)} \\
H_v(s) &= -1000 \cdot \frac{(s + 2\pi \cdot 5)}{s \cdot (s + 2\pi \cdot 2500)} \\
H_{id}(s) &= 500 \cdot \frac{(s + 2\pi \cdot 25)}{s \cdot (s + 2\pi \cdot 2500)} \\
H_{iq}(s) &= 1000 \cdot \frac{(s + 2\pi \cdot 5)}{s \cdot (s + 2\pi \cdot 2500)} \\
\left[d_{\text{offset\_min}},\ \ d_{\text{offset\_max}}\right] &= \left[-0.1,\ \ 0.1\right] \\
\left[i^*_{d2\_\text{min}},\ \ i^*_{d2\_\text{max}}\right] &= \left[-10,\ \ 10\right] \\
\left[m_{\text{min}},\ \ m_{\text{max}}\right] &= \left[0,\ \ 1\right].
\end{aligned}
\tag{7}
$$

V. CONCLUSIONS

A closed-loop control scheme for the three-level three-phase NPC dc-ac converter using the ONTV^2 PWM has been presented. The selected modulation allows using small dc-link capacitors leading to an improved performance of the closed-loop system. A specific control loop has been designed to speed-up the recovery from neutral-point voltage perturbations. The remaining part of the control is analogous to the control for a two-level converter, with an appropriate interfacing to the selected modulation, including an online estimation of the load angle at no extra cost. The good performance of the proposed control has been verified through simulation and experiments.

REFERENCES

[1] J. Rodríguez, J. Lai, and F. Peng, "Multilevel inverters: a survey of topologies, controls and applications," *IEEE Trans. Ind. Electron.*, vol. 49, pp. 724–738, Aug. 2002.

[2] L. Demas, T.A. Meynard, H. Foch, and G. Gateau, "Comparative study of multilevel topologies: NPC, multicell inverter and SMC with IGBT," in *Proc. IEEE Industrial Electronics Soc. Conf.*, vol. 1, 2002, pp. 828–833.

[3] A. Nabae, I. Takahashi, and H. Akagi, "A new neutral-point clamped PWM inverter," *IEEE Trans. Ind. Applicat.*, vol. IA-17, pp. 518–523, Sept./Oct. 1981.

[4] S. Ogasawara, and H. Akagi, "Analysis of variation of neutral point potential in neutral-point-clamped voltage source PWM inverters," in *Proc. IEEE Ind. Applicat. Soc. Annu. Meeting*, 1993, pp. 965-970.

[5] R. Rojas, T. Ohnishi, and T. Suzuki, "PWM control method for NPC inverters with very small dc-link capacitors," in *Proc. IPEC-Yokohama*, 1995, pp. 494–499.

[6] M. Cosan, H. Mao, D. Borojevic, and F. C. Lee, "Space vector modulation of three-level voltage source inverter," in *Proc. VPEC Seminar*, 1996, pp. 123–128.

[7] C. Newton, and M. Sumner, "Neutral point control for multi-level inverters: theory, design and operational limitations," in *Proc. IEEE Industry Applications Soc. Annu. Meeting*, 1997, pp. 1336–1343.

[8] D. H. Lee, S. R. Lee, and F. C. Lee, "An analysis of midpoint balance for the neutral-point-clamped three-level VSI," in *Proc. IEEE Power Electronics Specialists Conf.*, vol. 1, 1998, pp. 193–199.

[9] N. Celanovic and D. Boroyevich, "A comprehensive study of neutral-point voltage balancing problem in three level neutral-point-clamped voltage source PWM inverters," *IEEE Trans. Power Electron.*, vol. 15, pp. 242–249, Mar. 2000.

[10] Z. Tan, Y. Li, and M. Li, "A direct torque control of induction motor based on three-level NPC inverter," *IEEE Power Electronics Specialists Conf.*, vol. 3, 2001, pp. 1435-1439.

[11] J. Pou, D. Boroyevich, and R. Pindado, "New feedforward space-vector PWM method to obtain balanced ac output voltages in a three-level neutral-point-clamped converter," *IEEE Trans. Power Electron.*, vol. 49, pp. 1026–1034, Oct. 2002.

[12] Q. Song, W. Liu, Q. Yu, X. Xie, and Z. Wang, "A neutral-point potential balancing algorithm for three-level NPC inverters using analytically injected zero-sequence voltage," in *Proc. IEEE Applied Power Electronics Conf.*, vol. 1, 2003, pp. 228–233.

[13] S. Busquets-Monge, J. Bordonau, D. Boroyevich, and S. Somavilla, "The nearest three virtual space vector PWM — a modulation for the comprehensive neutral-point balancing in the three-level NPC inverter," *IEEE Power Electron. Lett.*, vol. 2, pp. 11-15, Mar. 2004.

[14] S. Busquets-Monge, S. Somavilla, J. Bordonau, and D. Boroyevich, "A novel modulation for the comprehensive neutral-point balancing in the three-level NPC inverter with minimum output switching frequency ripple," in *Proc. IEEE Power Electronics Specialists Conf.*, 2004, pp. 4226-4232.

[15] H. d. T. Mouton, "Natural balancing of three-level neutral-point-clamped PWM inverters," *IEEE Trans. Ind. Electron.*, vol. 49, pp. 1017-1025, Oct. 2002.

[16] J. Pou, P. Rodríguez, V. Sala, S. Busquets-Monge, and D. Boroyevich, "Algorithm for the virtual vectors modulation in three-level inverters with a voltage-balance control loop," in *Proc. European Conference on Power Electronics and Applications*, 2005, pp. 1-9.

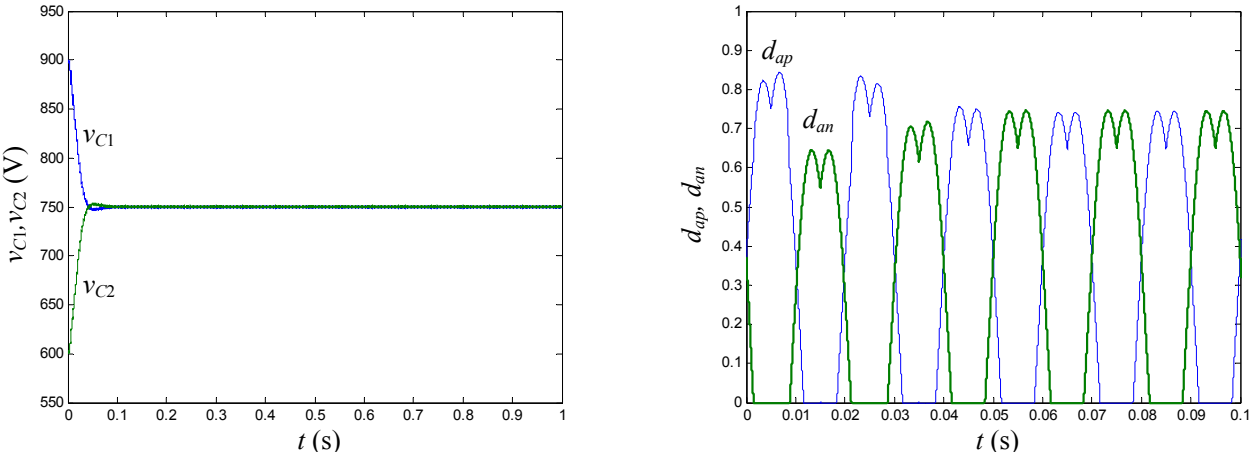

Fig. 4. Dc-link capacitor voltage balance recovery transient in the same conditions as in Fig. 2(a) but with the dedicated neutral-point voltage control activated. (a) Dc-link voltages v_{C1} and v_{C2}. (b) Phase a independent duty-ratios.

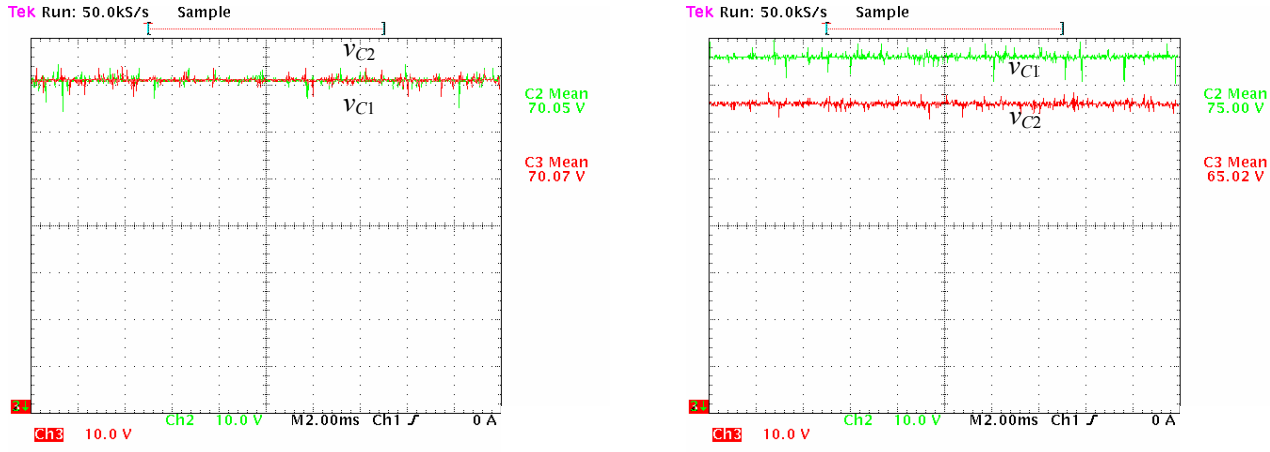

Fig. 5. Neutral-point voltage control performance in the following conditions: ONTV[2] PWM, $K = 0$, $V_{pn} = 140$ V, $m = 0.75$, $f_o = 50$ Hz, $f_s = 5$ kHz, $C_1 = C_2 = 1.1$ mF, $R_L = 16.5\ \Omega$, and $L_L = 5$ mH. (a) Control tuned to achieve $v_{unb} = 0$ V. (b) Control tuned to achieve $v_{unb} = -5$ V.

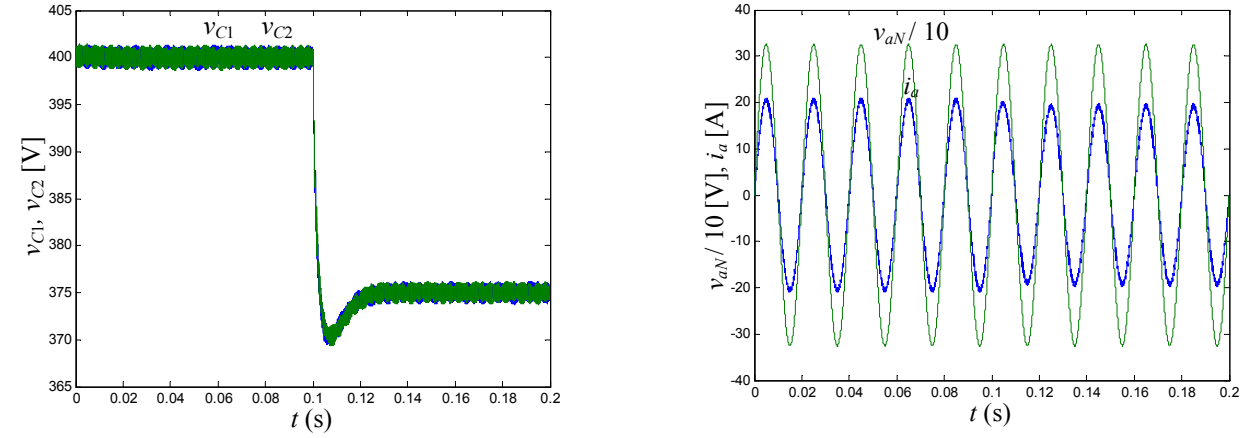

Fig. 6. Simulation results for a step in command v^*_{pn} at time = 0.1 s in the following conditions: $I = 12.5$ A, $C_1 = C_2 = 400$ μF, $L_L = 5$ mH, $V_{aN} = V_{bN} = V_{cN} = 230\ V_{rms}$, $f_o = 50$ Hz, and $f_s = 5$ kHz. (a) Dc-link voltages v_{C1} and v_{C2}. (b) Mains voltage v_{aN} and line current i_a.

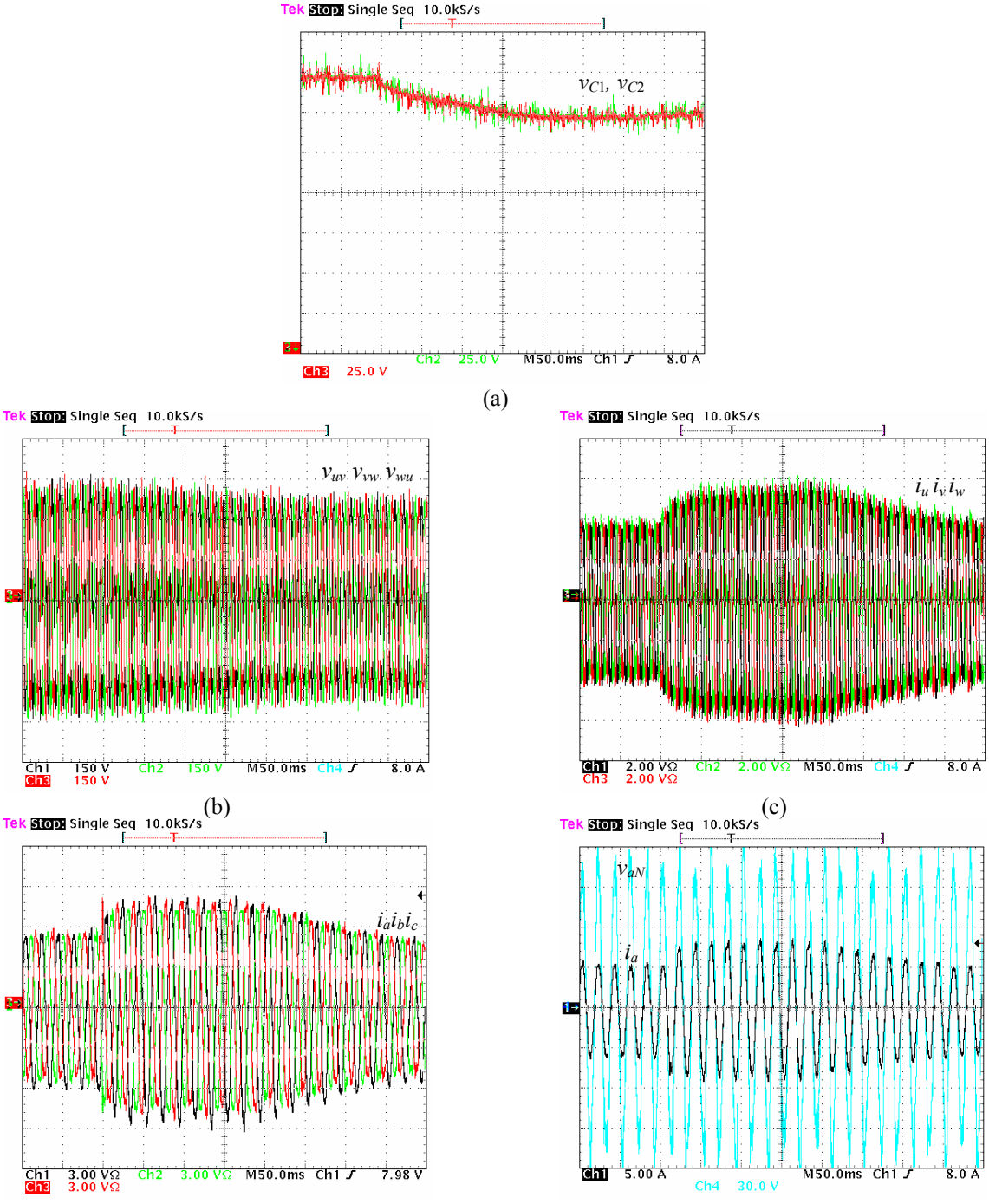

Fig. 7. Experimental results for a step in command v^*_{pn} from 340 V to 300 V (variation of rotor speed from 1577 rpm to 1396 rpm). Conditions: Rectified wind mill generator voltage, constant torque applied to the generator shaft = 10 Nm, L_S = 12.5 mH, $C_1 = C_2$ = 1.1 mF, L_L = 10 mH, $V_{aN} = V_{bN} = V_{cN}$ = 75 V_{rms}, f_o = 50 Hz, and f_s = 5 kHz. (a) Dc-link voltages v_{C1} and v_{C2} [25 V/div]. (b) Generator line-to-line voltages v_{uv}, v_{vw}, and v_{wu} [150 V/div]. (c) Generator currents i_u, i_v, and i_w [2 A/div]. (d) i_a, i_b and i_c [3 A/div]. (e) Mains voltage v_{aN} [30 V/div] and line current i_a [5 A/div].